Exercise 2.3
Sandpile

Pair **18**

Otto Salmela 1024166
Valtteri Silde 1009767

Report by *Otto Salmela*

Measurements performed **15.3.2024**
Report returned **28.4.2024**

Contents

1 Introduction

The goal of this exercise was to study the behavior and properties of a sandpile grown on a circular plate by examining the mass fluctuations of the pile as particles are dropped on it. The sandpile is grown from iron beads, and in this work four different measurements are conducted, each with different parameters, which were plate size and nozzle size. In addition to this, a computational experiment is conducted in which a sandpile is simulated. This report first covers the theory behind the phenomenon, after which the methodology behind the experiments is explored more in depth. Next, the results are presented and discussed, after which we conclude with a brief summary.

1.1 Self-organized criticality

Self-organized criticality is a property associated with dynamical systems where the system naturally evolves towards a critical state, meaning a state where the system is on the edge of stability and small perturbations can cause large effects [1]. The system approaches the critical state without the need for fine-tuning the parameters associated with the system, which comes apparent in systems that are not self-organizing critical, because to achieve a critical state the parameters of the system must be carefully adjusted. In the context of the sandpile, if we start from an empty plate and drop grains of sand at random locations, a pile will begin to form. Once the pile has formed, it will eventually reach a critical point where, if any more grains of sand (perturbations or noise) are added to the pile, it will slide off, possibly creating an avalanche in the process. This process is repeated by continuing to drop sand on the pile, thus making the pile repeatedly reach a critical point and creating avalanches in the process. In these types of systems, the physically observable quantities and noise often follow a power-law distribution [2]. The power-law distribution is proportional to $f^{-\alpha}$, where this represents the noise in the system and in our case the quantity which exhibits this proportionality is the flow of sand falling from the pile, or more generally the response of the pile to small random perturbations [1], [2]. This is often called the $1/f$ noise since α is in many physical systems close to one.

The sandpile naturally evolves towards a critical state as we drop sand on it, where avalanches start occurring and a consequence of this self-organized criticality is the existence of the critical angle and the angle of repose. The critical or maximum angle θ_m corresponds to the upper value after which the pile becomes unstable and an avalanche occurs, while the angle of repose θ_r corresponds to the value the angle drops down to after an avalanche [3]. Furthermore, the angle of repose is calculated after a large avalanche occurs [4].

2 Methodology

2.1 Test equipment and measurements

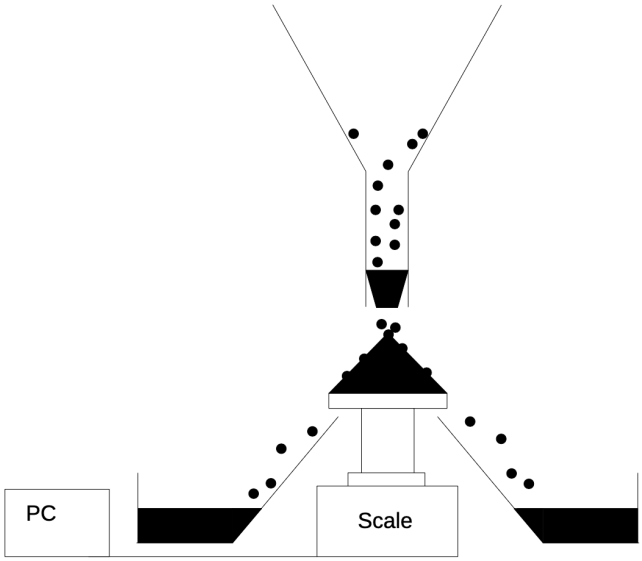

Figure 1: The measurement setup

The measuring equipment and setup can be seen in figure 1, where sand is dropped from a funnel onto a circular plate, on which a cone-shaped pile begins to form. The dropped iron beads range from 0,85 mm to 1,18 mm in diameter, so the figure above is not to scale [5]. The plate sits on a precision scale that measures the mass on top of it and stores this data on a computer as a function of time. The pile becomes unstable at some point, at which point an avalanche occurs and sand drips from the sides of the plate into the collection container.

In this work, four measurements are performed, two of which are with a 10 cm plate and the other two with a 13 cm plate. A measurement is performed on each plate with two nozzles of different sizes, 6,5 mm and 7,5 mm, which are placed in the mouth of the funnel, as seen in figure 1. In this way, we are able to manipulate the flow rate and analyze how both the size of the nozzle and the plate affect the pile behavior and the probability density distribution of the avalanche size.

2.2 Determining coefficients and angles

After the measurements, the data is analyzed with MATLAB (see Appendix 1). First, we need to determine how fast the measuring device saves data. This was done with a test measurement that lasted 10 seconds, and 92 data points were saved, meaning the time between measurements is approximately 0,11 seconds. Next, the flow rate of the sand is approximated, which is used in calculating the size of the avalanches, by taking a steadily increasing part of the mass in between avalanches. After this, we need to iterate over the entire measurement and detect all avalanches and their sizes. This is done by examining when the time derivative of mass goes negative, and then calculating the mass difference until the time derivative turns positive again. With this, we end up with a vector where each element corresponds to one avalanche. With this vector, the avalanche size distribution can be divided into a number of bins, which are uniformly distributed on a log-log scale, to produce a good probability density distribution on this scale. If any of these bins are empty, meaning there were no avalanches

in a particular size interval, they will be excluded from the log-log scale figures since they would produce $-\infty$.

$$p(m) = Am^{-\alpha} \tag{1}$$

With the avalanche size distribution divided into bins, the cumulative and probability density distributions can be created, which will be shown both on linear and logarithmic scales. The power-law discussed in the introduction in our case takes on the form of equation (1), where m is the mass of the avalanche and A and α are parameters we would like to determine. Since the flow of sand falling from the pile at least approximately follows the power-law, we use this to detect a part of the probability density where it seems linear in log-log scale, to which a line can be fitted with the MATLAB "fit" function.

$$\log p = -\alpha \log m + \log A \tag{2}$$

$$\Delta \log A = \left| \frac{d}{dA} (\log A) \right| \Delta A \tag{3}$$

$$\Delta A = A \ln(10) \, \Delta \log A \tag{4}$$

The power-law on log-log scale can be seen in equation (2), so the coefficients and errors given by the "fit" function will correspond to $-\alpha$ and $\log A$. The error for α will be the same as the one given by the function, and the error for A can be calculated from the exact differential given in equation (3), which gives us the error for A shown in equation (4).

To determine the critical angles and the angles of repose, we will have to get an estimate for the height of the pile corresponding with the maximum weight of the pile and the weight of the pile after a large avalanche. Approximating the pile as a cone, one can use the equation for the volume of a cone and solve for height, which yields us equation (5)

$$h = \frac{3m}{\rho \pi r^2}, \tag{5}$$

where m is the mass of the pile, ρ is the density of the pile, and r is the radius of the plate. For determining the critical angle θ_m, the maximum observed mass in the measurement is used, and for the angle of repose θ_r, the maximum mass subtracted by the biggest observed avalanche size is used since the angle of repose corresponds to the angle to which the pile returns after a large avalanche occurs. The angles are determined from the simple trigonometry of the pile using equation (6).

$$\theta = \arctan\left(\frac{h}{r}\right) \tag{6}$$

The density of iron is approximately 7860 $\frac{kg}{m^3}$, but iron beads are much less dense compared to pure iron [6]. For this, we will do a very rough approximation that the density of the pile is about 75% of this. This approximation was made because it yields us heights that correspond well with the observed heights of the piles after the measurements, which were around 3 cm.

2.3 Simulation

In addition to the measurements, a simulation is performed, the results of which are compared with the results obtained from the measurements. The calculation model used in this work is called a Cellular Automaton (CA), and it works as follows [5].

The most important part of this model is the height matrix, which describes the height at different points of the pile, at different simulation steps. Due to the symmetry of the situation, it is enough to simulate only one quarter of the pile. At each simulation step, one grain of

sand is dropped into a random location in the pile. This location is determined by utilizing the MATLAB function "rand," which returns a random number uniformly from the interval (0,1) [7].

$$z = R \cdot rand \cdot e^{i\frac{\pi}{2} \cdot rand} \tag{7}$$

Equation (7) gives us a complex number with magnitude ranging from 0 to R and phase ranging from 0 to $\frac{\pi}{2}$ (since only a quarter of the pile is simulated), where R is the radius of the simulated pile and rand is the number returned by the "rand" function. The real and complex parts of z are then used to determine the spot in the height matrix where the grain of sand is dropped. Each radius and phase is equally likely, but since larger radii cover a larger area, the probability distribution will be denser around the center of the pile.

After a grain of sand is dropped, the model then calculates a matrix of local slopes based on the height matrix. If the local slope exceeds the critical slope, which can be altered in the simulation, one grain is moved downward in the y-direction and another in the x-direction. This is done until the pile is stabilized again, after which the mass of the pile is stored and a new simulation step starts. The model keeps track of avalanches and their sizes similarly to the experimental part of this work, so the same methods described in Section 2.2 can be used to determine distributions and coefficients for the power-law, but critical angles and angles of repose are not calculated for the simulation pile. The code associated with the simulation can be seen in Appendix 2.

3 Results

Table 1: The obtained results from the measurements

Plate (cm)	Nozzle (mm)	A	ΔA	α	$\Delta\alpha$	θ_m (°)	θ_r (°)	δ (°)
10	6,5	0,0763	0,0157	0,4415	0,1485	27,9041	26,6812	1,2229
10	7,5	0,1198	0,0417	0,6045	0,2054	27,7531	26,2819	1,4712
13	6,5	0,0970	0,0390	0,8652	0,2782	25,9991	25,1166	0,8824
13	7,5	0,1286	0,0422	0,6659	0,1598	27,1348	26,2063	0,9285

The obtained results from all the measurements are gathered and shown in Table 1, along with the errors for the coefficients given by the MATLAB function "fit". A more in depth analysis of each measurement is done in the following subsections. The errors and angles for all the measurements seen in the table are calculated with the methods described in Section 2.2.

3.1 10 cm diameter plate

3.1.1 6,5 mm nozzle

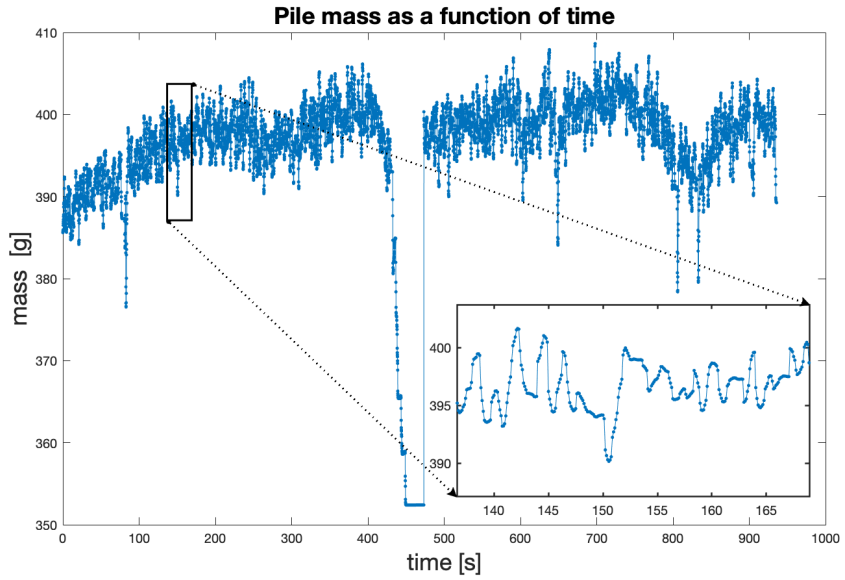

Figure 2: The mass of the pile as a function of time

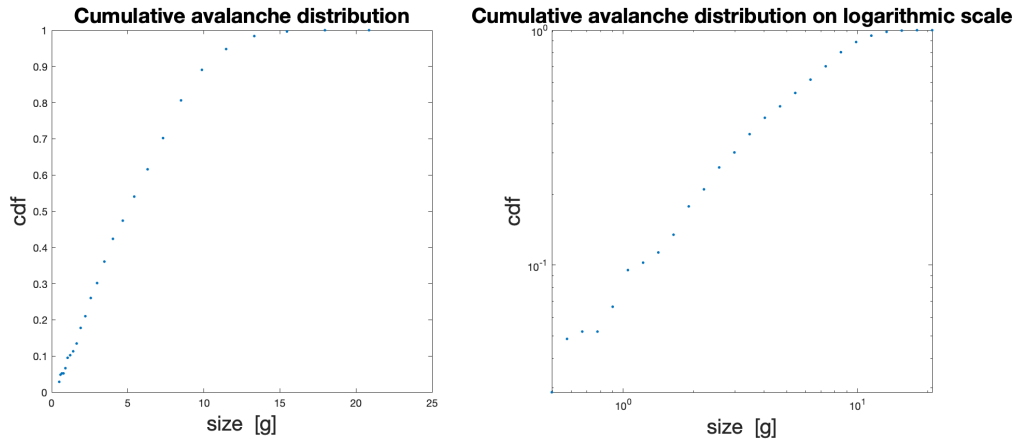

Figure 3: The cumulative avalanche size distribution both on linear (left) and logarithmic (right) scales

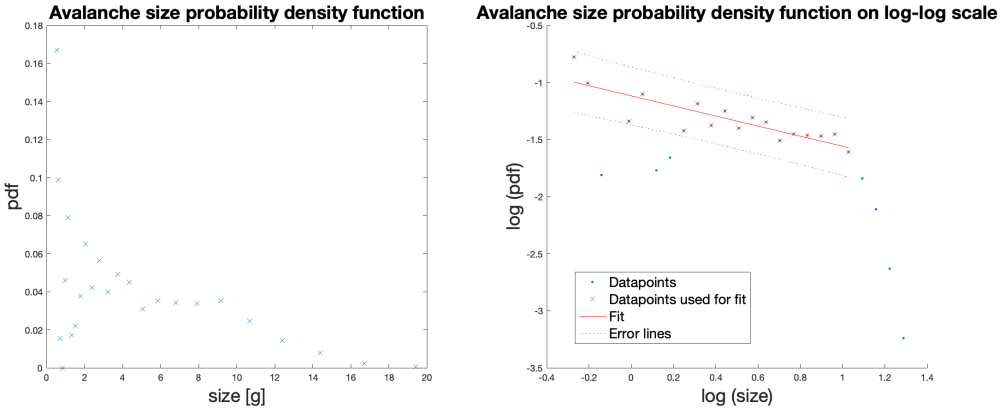

Figure 4: The avalanche size probability density distribution both on linear (left) and log-log (right) scales

This measurement was performed for approximately 15 minutes and 558 avalanches were detected. There was a discontinuity in the middle of the measurement, which can be seen in figure 2, due to a piece of tape clogging the nozzle. This discontinuity is not included in the determination of the avalanche vector and probability distributions. The mass of the pile as a function of time from the entire measurement and a zoomed interval are shown in figure 2. This interval was chosen as it showcases well the behavior of the pile during the measurement, and the data is easily readable. The datapoints are shown as dots, and they are connected with a line to improve readability and aid in spotting avalanches. Figures for the other measurements will be shown in the same manner.

In figures 3 and 4, the cumulative and probability density distributions can be seen for this experiment. The number of bins was ultimately chosen to be 25, because with this choice, the number of empty bins is minimal while also giving us a sufficient amount of datapoints for fitting and analysis. This bin choice is used for all the experiments and figures. Both are shown on linear and logarithmic scales. The fit can be seen in figure 4 on the right, where the right end is excluded from the fit since it doesn't behave linearly with respect to the rest of the data. Also, three outliers are excluded since they are significantly distant from every other datapoint. Outliers corresponding to smaller avalanches are expected due to errors with precision in the measuring device, but datapoints fitting well with the linearity of the middle-sized avalanches are included in the fit [8]. These reasonings for exclusion also apply to the other measurements as well. The fit in log-log scale gives us values $-\alpha = -0{,}4415$ and $\log A = -1{,}1174$, which are used to calculate the coefficients in Table 1.

3.1.2 7,5 mm nozzle

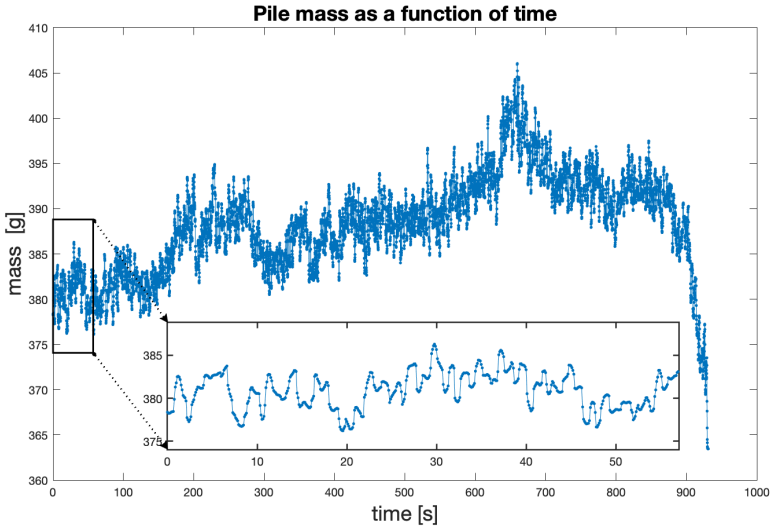

Figure 5: The mass of the pile as a function of time

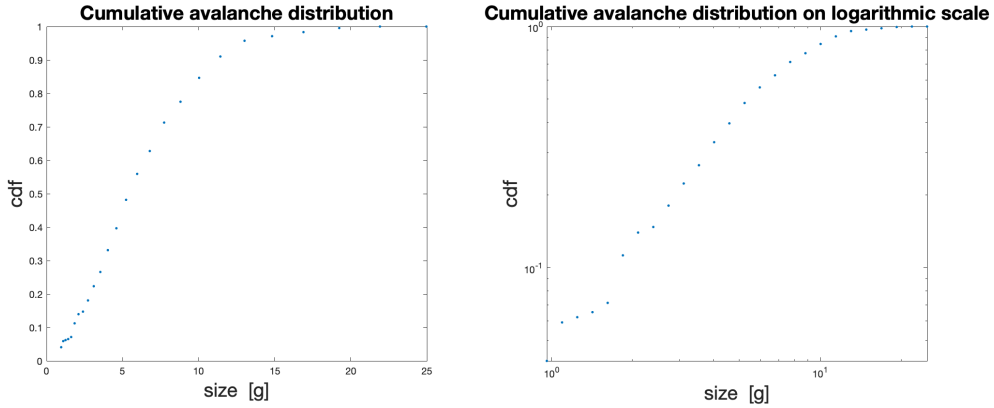

Figure 6: The cumulative avalanche size distribution both on linear (left) and logarithmic (right) scales

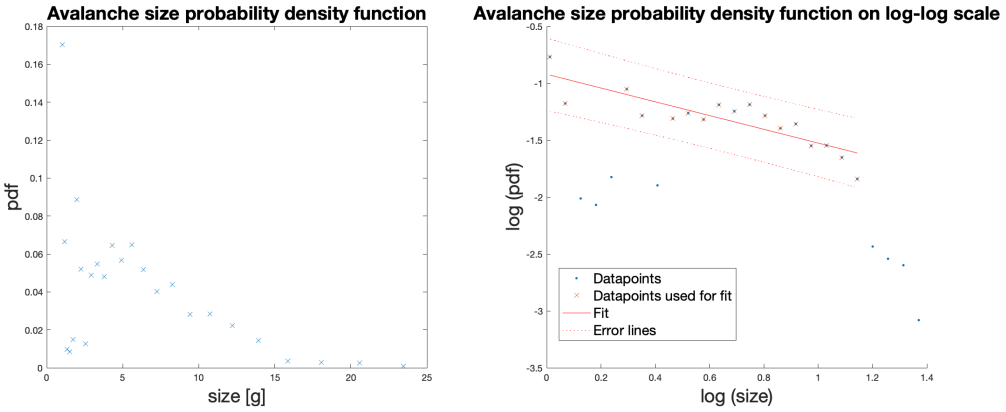

Figure 7: The avalanche size probability density distribution both on linear (left) and log-log (right) scales

This measurement was performed again for approximately 15 minutes and 659 avalanches were detected. The end of the data included a part when the sand wasn't flowing, which can be seen in figure 5, so this was excluded from determining the distributions. The mass of the pile as a function of time from the entire measurement and a zoomed interval are shown in figure 5, which shows the behavior of the pile during the measurement. This interval was chosen for the same reasoning as before.

In figures 6 and 7, the cumulative and probability density distributions can be seen for this experiment, and again both are shown on linear and logarithmic scales. The fit can be seen in figure 7 on the right, where the right end is again excluded, and this time four clear outliers are excluded. The fit in log-log scale gives us values $-\alpha = -0{,}6045$ and $\log A = -0{,}9217$, which are again used to calculate the coefficients in Table 1.

3.2 13 cm diameter plate

3.2.1 6,5 mm nozzle

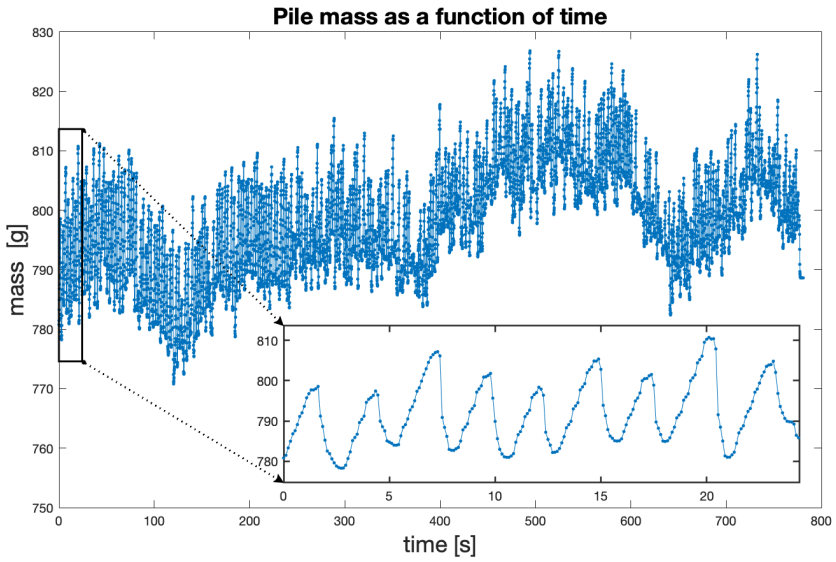

Figure 8: The mass of the pile as a function of time

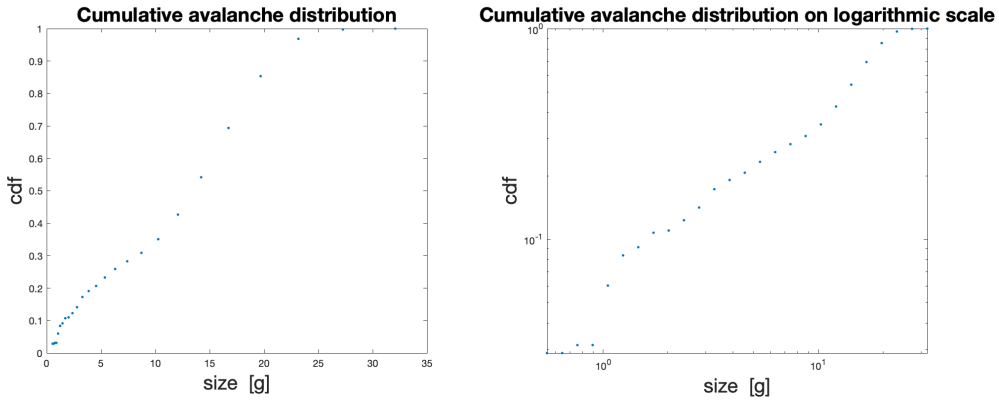

Figure 9: The cumulative avalanche size distribution both on linear (left) and logarithmic (right) scales

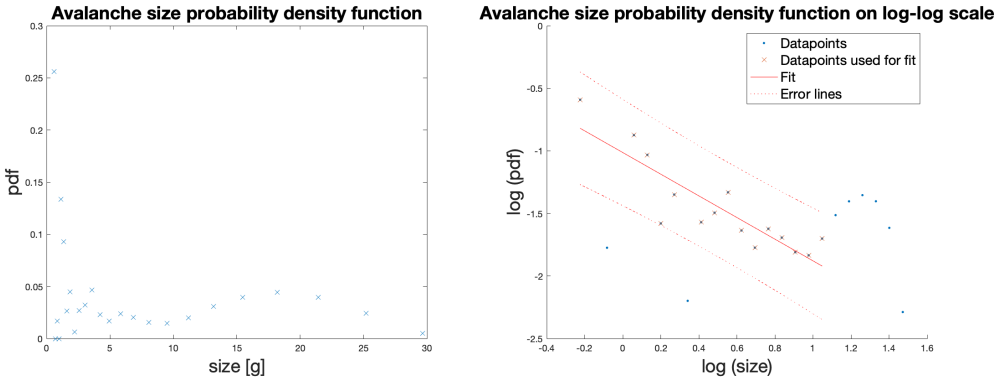

Figure 10: The avalanche size probability density distribution both on linear (left) and log-log (right) scales

This measurement was performed for approximately 13 minutes and 382 avalanches were detected. The mass of the pile as a function of time from the entire measurement and a zoomed interval are shown in figure 8, which shows the behavior of the pile during the measurement. This interval was chosen for the same reasoning as before.

In figures 9 and 10, the cumulative and probability density distributions can be seen for this experiment, and again both are shown on linear and logarithmic scales. The fit can be seen in figure 10 on the right, where the right end is again excluded since it behaves abnormally, and this time two clear outliers are excluded. The fit in log-log scale gives us values $-\alpha = -0{,}8652$ and $\log A = -1{,}0133$, which are again used to calculate the coefficients in Table 1.

3.2.2 7,5 mm nozzle

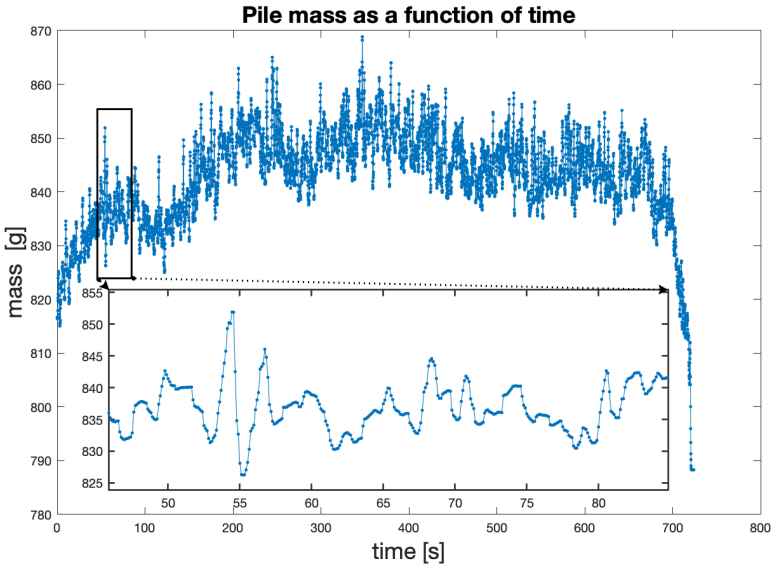

Figure 11: The mass of the pile as a function of time

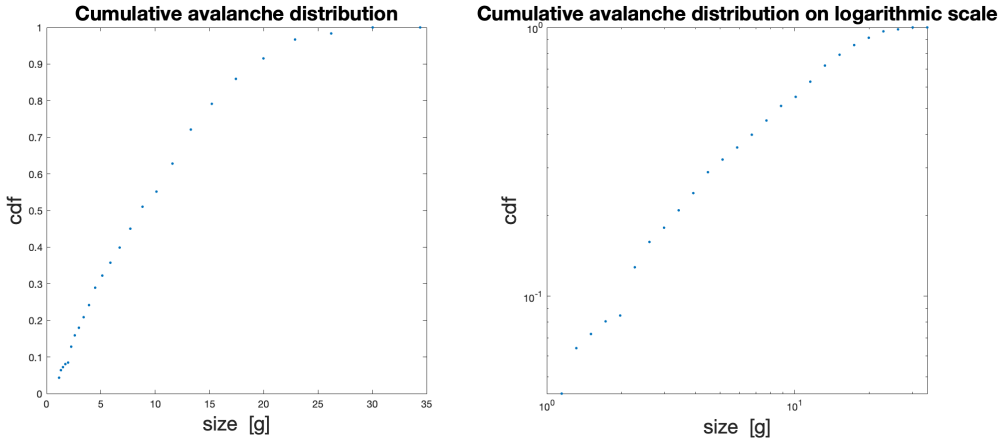

Figure 12: The cumulative avalanche size distribution both on linear (left) and logarithmic (right) scales

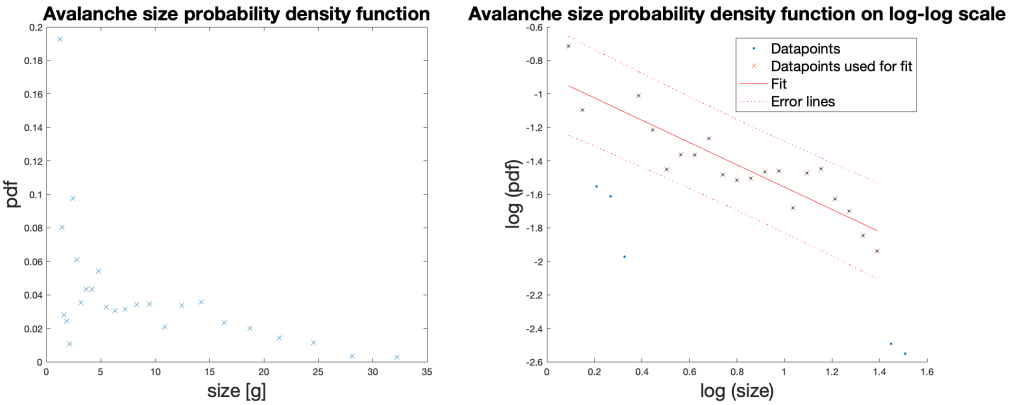

Figure 13: The avalanche size probability density distribution both on linear (left) and log-log (right) scales

This measurement was performed for approximately 12 minutes and 484 avalanches were detected. The end of the data again included some data when the sand wasn't flowing, so this was excluded from determining the distributions. The mass of the pile as a function of time from the entire measurement and a zoomed interval are shown in figure 11, which shows the behavior of the pile during the measurement. This interval was chosen for the same reasoning as before.

In figures 12 and 13, the cumulative and probability density distributions can be seen for this experiment, and again both are shown on linear and logarithmic scales. The fit can be seen in figure 13 on the right, where the right end is again excluded, and this time three clear outliers are excluded. The fit in log-log scale gives us values $-\alpha = -0{,}6659$ and $\log A = -0{,}8908$, which are again used to calculate the coefficients in Table 1.

3.3 Simulations

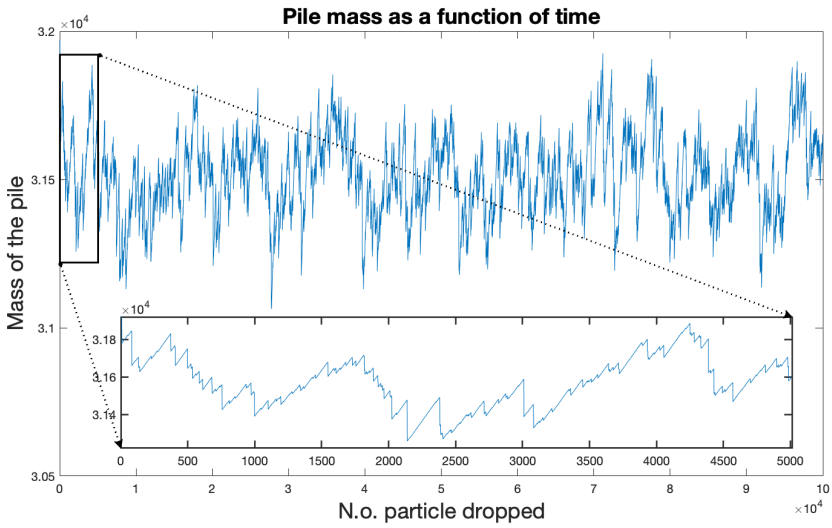

Figure 14: The unit mass of the pile as a function of time step for the unit size 50 plate

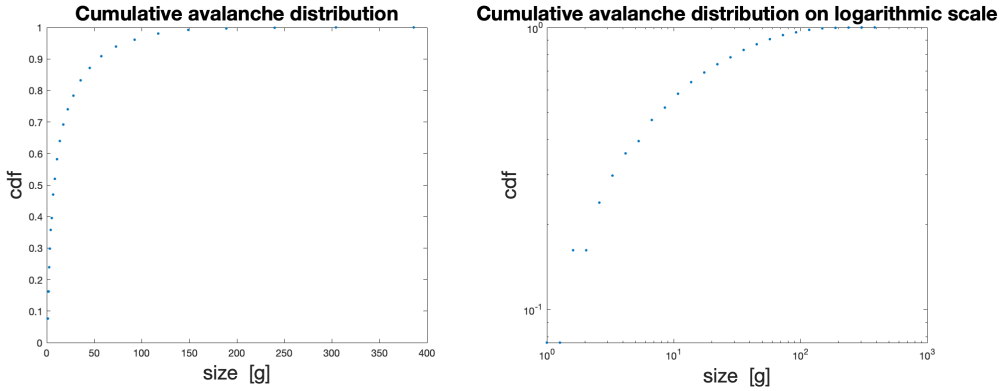

Figure 15: The cumulative avalanche size distribution both on linear (left) and logarithmic (right) scales for the unit size 50 plate

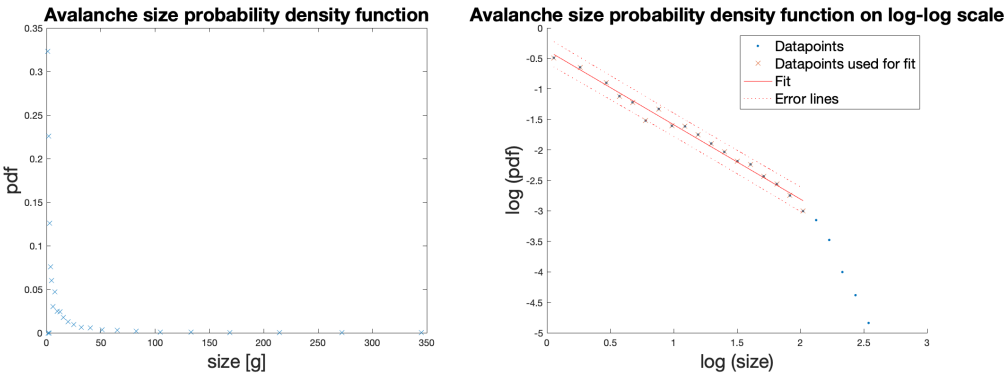

Figure 16: The avalanche size probability density distribution both on linear (left) and log-log (right) scales for the unit size 50 plate

Table 2: The obtained results from the simulations

Plate size	A	ΔA	α	$\Delta\alpha$	Avalanche count
25	0,5462	0,1435	1,3608	0,0978	6123
50	0,4288	0,0929	1,2173	0,0745	3806
100	0,4882	0,1197	1,1538	0,0764	2275
150	0,4694	0,1554	1,0954	0,0988	1757
200	0,5090	0,1697	1,1001	0,0893	1375

All of the simulations were performed for 100 000 time steps to gain a sufficient amount of data and the results from the simulations can be seen in table 2. The size of the plate was varied to see if it would have any effect on the power-law parameters and the critical slope was also experimented with, but varying this seemed to have little to no effect. Because of this, a critical slope of 3 was used for the results obtained in table 2, because this seems to make the most sense in the context of the simulation since the simulation always reduces the number of grains by 2 when the slope is large enough (meaning the pile likes to remain conical with unit size slope). The avalanche count, which determines the size of the dataset, drops significantly as the size of the plate is increased, which makes sense as the size of the pile is increased, more grains of sand need to be dropped to produce an avalanche. The dataset sizes are however sufficiently large to produce good distributions for all the simulations and much bigger than with the actual measurements.

Figures for one of the simulations (size 50 plate) are presented to visualize the behaviour and results of the simulations, but figures from other simulations are not presented since they look approximately the same as with the unit size 50 plate. The plate size for the figures was chosen to be 50 because on average the iron beads are approximately 1 mm in diameter, so the simulated plate would be approximately 5 cm in radius, which corresponds well to the actual plates which were used. The mass of the pile as a function of time as well as a zoomed interval for the size 50 plate is shown in figure 14, which gives an example of the behaviour of the piles during the simulations. The datapoints in figure 14 are not indicated with dots since the data is approximately continuous.

In figures 15 and 16, the cumulative and probability density distributions can be seen for the plate size 50 simulation, and again both are shown on linear and logarithmic scales. With smaller avalanche sizes, some bins are empty, which can be seen as a discontinuity in the cumulative distributions in figure 15. These are due to the bins being uniformly distributed in logarithmic scale, so some smaller bins do not contain whole numbers, thus leaving them empty since one grain of sand has mass of one, meaning the avalanche sizes can only be whole numbers. These are excluded from the fit and the figure since they are $-\infty$ in log-log scale. The fit can be seen in figure 16 on the right, where the right end is again excluded due to the same reason as in the experimental measurements. The probability density distributions for all the simulations looked approximately like the one presented in figure 16, where the right end sloped downward.

4 Discussion

4.1 Interpretation of the results

From Table 1, we see that the values for the coefficient α are significantly off from what would be expected for self-organized critical systems, which would be around one as found in [1], indicating that the theory of self-organized criticality might not be entirely sufficient when analyzing physical sandpiles. The biggest differences come with the smaller plate, and the closest result obtained is with the 13 cm plate with the 6,5 mm nozzle. The values for A however, seem to be following a pattern. For the 6,5 mm nozzle, A is significantly lower with

both plates than with the 7,5 mm nozzle, and also with the larger plate, the values seem to be slightly larger than with their smaller counterparts.

Let's now consider what these results actually mean. As α grows larger, the probability density distribution will become more weighted towards smaller avalanches, and as A grows, the entire distribution effectively gets shifted to the right. This would suggest that with larger plates smaller avalanches are more likely, and with the 7,5 mm nozzle larger avalanches become more likely. However, the entire distribution is not taken into account here, and the data is only considered through the power-law and self-organized criticality.

The distribution for the 13 cm plate with the 6,5 mm nozzle seen in figure 10 behaves abnormally compared with the others, where a rise in the likelihood of large avalanches is seen. This can also be seen in figure 8, where large avalanches can be seen happening periodically, which is very different from the other mass figures, where smaller avalanches happen much more often. This is in line with the results in [4], and it happens due to self-organized criticality not being entirely applicable anymore and the characteristic earthquake model becoming a better approximation, where large avalanches happen periodically. This happens when the ratio between the size of the grains of sand and the plate size becomes small enough. In the same paper, they found that the diameter of funnels had no remarkable effect on the results, but in our experiment, it clearly did. For example, the larger plate with the larger funnel doesn't meaningfully exhibit the earthquake model, while the smaller funnel does. This could be because the 13 cm plate is only just above the threshold for the earthquake model to take effect, and as the flow rate is increased, more noise and perturbations happen in the pile, making the self-organized criticality behavior become active again [3]. All of the measurements also have outliers corresponding to smaller avalanches, which could be indicative of the self-organized criticality model being insufficient, but also the precision of the measuring apparatus could be the reason behind this.

As for the critical angles and angles of repose, the results are with good accuracy the same regardless of plate and nozzle size. There is a slight difference in the 13 cm plate with the 6,5 mm nozzle, but it is within reason, and this measurement exhibited the most dissimilarities when compared with the others, so it is not surprising that it also differs here. As for the differences in the angles, the results for the smaller plates are much more in line with the reference value, which is around 2° [4]. This could also be indicative of the fact that self-organized criticality applies worse with the larger plates.

Considering everything, interpreting the results proves to be quite difficult because of the large errors associated with the obtained results (these are discussed more in depth in the next section) and the complexity of the physics of the situation. Nevertheless, the most important conclusions we can draw from the results, in my opinion, are that with larger plates, the self-organized criticality model becomes less valid, and with larger nozzles, more perturbations happen in the pile. If these perturbations are meaningful in the context of the pile, for example they might not be if we considered a very large pile, they could cause avalanches to happen more frequently. This is seen when comparing the two measurements with the larger plate with each other and especially when comparing figures 8 and 11, where with the larger nozzle we see avalanches happen much more frequently and with much more variance in the sizes of the avalanches.

4.2 Reliability of the results

When considering the errors shown in table 1, the reliability of the results is taken into question. The errors are consistently about a third of the actual values, which is very significant. For A, we do not have any reference values as to what they could be, but they seem to be the most consistent out of all the values. As for α, the results differ from what was expected by a lot, and even taking the errors into account, some of the values do not get close to what was expected for self-organized critical systems. Also, the calculated differences for the critical

angles and angles of repose differ significantly from what was expected, which could be an approximation error but nevertheless, the observed heights after the measurements match with relatively good accuracy with what was calculated.

There could be, and most likely are, multiple different reasons for the errors seen in the measurements. The first major reason has to do with the nature of the measurements and the measuring apparatus. The scale used most likely has trouble calculating small differences in weight that accurately reflect the state of the pile, especially when iron beads are continuously dropped on the pile. Because of this, smaller avalanches could be lost in the noise of the continuous flow. In addition to this, the theory of self-organized criticality might not be entirely valid, especially with the larger plates. The conclusion of the results gotten in [3] was that sand does not behave as predicted by the power-law and self-organized criticality, and granular matter in general, does not show this type of behavior.

Nevertheless, in my opinion, examining the behavior of the pile through self-organized criticality is at the very least partly valid, especially with the smaller plates, and the errors associated are due to other errors such as precision errors. The measurements could thus be improved by for example upgrading the measurement apparatus, but most importantly by conducting the measurements in a more controlled manner, where the beads are dropped with a more controlled approach. Also, the length of the measurements could be extended to obtain more data and better results.

4.3 Comparison of the simulation and the real experiment

From table 2 we can see that as we increase the plate size, α becomes smaller, meaning larger avalanches become more likely. However, α doesn't seem to decrease linearly, but it approaches values of around 1,1 with larger plate sizes. As for the coefficient A, no significant deductions can be made as to how it behaves based on plate size from the attained results.

When comparing the results from the simulations with the results from the measurements in Table 1, one can see clear differences in both the coefficients of the power-law. Both of the coefficients are larger with the simulations, but most importantly, α is closer to what would be expected from self-organizing critical systems when compared with the experimental results, especially with larger simulation plates. Furthermore, when we compare the value of α from the simulation of unit size 50 with the actual measurements with the 10 cm plate (which should correspond to each other well as explained in section 3.3), we notice that the simulation value is much larger.

The simulation differs meaningfully from the real experiment; for example the simulation is based on self-organized criticality and does not exhibit meaningfully the signs of the characteristic earthquake model even when the size of the plate is increased by a lot, while with one of the 13 cm plate measurements larger avalanches started to happen periodically. If we only look at the coefficients α, we see that with the simulation it decreases as plate size is increased and in the actual measurements we see the opposite effect. Additionally, the only thing determining whether or not a particle falls downward in the simulation is the local angle in the pile. In reality, this is a very complex relationship that has to do with multiple variables, such as different forces, stress, and vibrations in the pile.

The simulation also exhibits some similarities with the actual measurements. For example, the distribution for where the grains of sand are dropped becomes denser toward the middle of the pile and in the actual measurements they were dropped in the middle. Additionally, in figure 16, we can see the probability density in log-log scale drop as the size of the avalanche increases (this was true for all the simulations), much like in actual measurements. These similarities indicate that the methods of the simulation at least somewhat reflect reality.

5 Conclusions and summary

In conclusion, this work studied the self-organizing criticality properties of sandpiles, such as probability distributions of avalanche size. The results from this exercise were significantly inaccurate, but some meaningful results and conclusions were obtained with the help of previous experiments and results. These included the characteristic earthquake model taking into effect with larger plate sizes (ie. when the ratio between the size of the grains of sand and the plate size is small enough), larger perturbations (meaning a larger funnel) making smaller avalanches more likely again and self-organizing criticality being more applicable with smaller plates. The differences between the critical angles and angles of repose were also closer to the reference value with the smaller plates, whereas not much can be deduced based solely on the power-law coefficients attained, except that values of α differed significantly from the reference value. The simulation methods and results mostly contradict the ones of the actual measurements, but there were some similarities, such as the shape of the probability density distribution in log-log scale and similar distributions for where the sand is dropped. The inaccuracies could be improved by tackling the aforementioned problems and, for example, conducting the experiment in a more controlled manner, by for example calibrating the plate to ensure it is horizontal and coupling the funnel and plate together so that the sand is dropped perfectly center. This way, the precision errors could be mitigated. The obtained results indicate the need for further improvement of the experimental methods and consideration of other theories pertaining to sandpiles to enhance accuracy and deepen our understanding of self-organized critical systems such as earthquakes and avalanches.

References

[1] P. Bak, C. Tang, K. Wiesenfeld, Phys. Rev. A 38, 364-375 (1988), 25.3.2024

[2] P. Bak, C. Tang, K. Wiesenfeld, Phys. Rev. Lett. 59, 381-384 (1987), 25.3.2024

[3] S. R. Nagel, Rev. Mod. Phys. 64, 321-325 (1992), 25.3.2024

[4] N. Yoshioka, Earth Planets Space 55, 283-289 (2003), 25.3.2024

[5] Aalto University, "Working instructions: Examination of the granular material flow" (PHYS-C0310 course material, Työ_2p5_sand_pile.pdf, 9.1.2017), 23.3.2024

[6] P. Evans, "Density of metals" (18.5.2015), https://theengineeringmindset.com/density-of-metals/, 24.3.2024

[7] MathWorks, "rand", https://se.mathworks.com/help/matlab/ref/rand.html, 24.3.2024

[8] Aalto University, "PHYS-C0310 - 2.4 Hiekkakasa - Mittaus 2" (PHYS-C0310 course video), https://aalto.cloud.panopto.eu/Panopto/Pages/Viewer.aspx?id=46c122a4-23bb-47e4-bd8d-ab9800af78cc&start=206.982239, 24.3.2024

Appendix

Appendix 1: MATLAB code for the experiments

```
%This is code for only one of the experiments. For the others, the file
%name, flow rate calculation indexes, start and end points, indexes
%to exlude from the fit and plate radius could possibly need to be changed
clear;

clear Nx imp cal h;

% Reading the data
imp=dlmread('plate_100mm_nozzle7_5mm.txt');
virt=imp(:,1);
t = (0:(1/9.2):(length(imp) - 1)/9.2);
max_mass = max(virt)*10^(-3);

% The mass-time figure
figure();
plot(t, virt, '.-')
title("Pile mass as a function of time",'FontSize',18);
xlabel('time [s]','FontSize',18)
ylabel('mass  [g]','FontSize',18)
zp = BaseZoom();
zp.run;

% Setting zero
virt=virt-min(virt);

Nx=length(virt);
```

```
t=linspace(1,Nx,Nx);


% Calculating flow rate from a steadily increasing part inbetween
% avalanches
i_min = 4888
i_max = 4898

% note! here the stream is grams per index
dm = virt(i_max) - virt(i_min)
di = i_max - i_min
stream = dm/di
% Mass time derivative
for i=1:Nx-1

   Dvirt(i)=virt(i+1)-virt(i);

end

% Finding avalanches

sp=1; % Start point
ep=8300; % End point

i=sp;
j=1;
k=1;

while i<ep

    virt2(i)=virt(i);

    if and(Dvirt(i)<0,Dvirt(i+1)<0) % If avalanche begins

        j=1;
        while Dvirt(i+j)<0 % Avalanche continues until
                           % mass isn't decreasing anymore
            virt2(i+j)=virt(i)+stream*j;
            j=j+1;
        end

        i=i+j;
        virt2(i)=virt(i);

        ava(k)=-virt2(i)+virt2(i-1); % The size of the avalanche
                                     % to the ava-vector
        Tava(k)=i; % The time when it happened
        k=k+1;


    else % If no avalanche, we move forward
```

```
        i=i+1;
    end

end

min_value = min(ava);
max_value = max(ava);
num_bins = 25;
% Define the range of exponents for the logspace
exponents = linspace(log10(min_value), log10(max_value), num_bins+1);

% Calculate the bin edges
bins = 10.^exponents;
count = histc(ava, bins);

% ava cumulative increasing
figure;
subplot(1, 2, 1);
cumulative = cumsum(count);
plot(bins, cumulative/cumulative(end), '.');
hold on;
title("Cumulative avalanche distribution",'FontSize',20);
xlabel('size  [g]','FontSize',20);
ylabel('cdf','FontSize',20);

% loglog cumulative
subplot(1, 2, 2);
loglog(bins, cumulative/cumulative(end), '.');
title("Cumulative avalanche distribution on logarithmic scale",'FontSize',20);
xlabel('size  [g]','FontSize',20);
ylabel('cdf','FontSize',20);

% ava pdf
figure;

subplot(1, 2, 2);
pdf = count(1:(end-1))./(bins(2:end) - bins(1:(end-1)));
binlog = log10((bins(2:end) + bins(1:(end-1)))/2);
pdflog = log10(pdf/sum(pdf));

hold on;
% ava pdf loglog
loglog(binlog, pdflog, '.');

% Exclude the right part
x = binlog(:,1:21);
y = pdflog(:,1:21);

% Exclude outliers and -Inf indexes
index_to_exclude = [3 4 5 8];
inf_indexes = find(y == -Inf);
```

```
% Remove -Inf
x(:, inf_indexes) = [];
y(:, inf_indexes) = [];

% Remove outliers
x(:, index_to_exclude) = [];
y(:, index_to_exclude) = [];

title("Avalanche size probability density function on log-log scale",'FontSize',20);
f = fit(x',y', 'poly1');
plot(f,x,y,"x",'predobs');
xlabel('log (size)','FontSize',20);
ylabel('log (pdf)','FontSize',20);
legend("Datapoints", "Datapoints used for fit","Fit", "Error lines",'FontSize',15);

hold off;

% ava pdf linear scale
subplot(1, 2, 1);
plot((bins(2:end) + bins(1:(end-1)))/2,pdf/sum(pdf), 'x');
title("Avalanche size probability density function",'FontSize',20);
ylabel('pdf','FontSize',20);
xlabel('size [g]','FontSize',20);

% Calculating heights corresponding to the different angles
ci = confint(f);
rho = 7860*0.75;
r = 0.10/2;
max_pile_height = 3*max_mass/(rho*pi*r^2)
rep_pile_height = 3*(max_mass-max(ava)*10^(-3))/(rho*pi*r^2)

% Calculating angle of repose, critical angle, their difference,
% the coefficients and their errors
Alog = f.p2;
A = 10^Alog
dA = A*log(10)*abs(ci(1,2)-ci(2,2))/2
alpha = -f.p1
dalpha = abs(ci(1,1)-ci(2,1))/2
crit_angle = rad2deg(atan(max_pile_height/r))
rep_angle = rad2deg(atan(rep_pile_height/r))
diff = crit_angle-rep_angle
```

Appendix 2: MATLAB code for the simulation

```
% Simple Cellular Automata model for sandpile
% Created by Akusti Jaatinen

clear;

Nx=50;   % Size of the pile
```

```
Np=100000; % N.o. particles to drop
Zc=3;   % Critical slope

PI=1000; % Plot interval
PA=0; % Avalanche to plot (0=don't plot)

C=zeros(Nx,Nx);
for i=1:Nx
for j=1:Nx

r=sqrt((Nx-i)^2+(Nx-j)^2);
if r<Nx
C(i,j)=1;

% Start from H ~ -r + noise
H(i,j)=round((Nx-r)*Zc*0.6*(1+0.1*rand));
end
end
end

H=C.*H;

DA=0; % Avalanche distribution
NA=0; % Number of avalanches

% Matrices for calculating the slopes
A=sparse(-diag(ones(Nx-1,1),-1)+diag(ones(Nx,1),0));
B=transpose(A);

T=sqrt(-1)*pi/2; % i times the angle


M(Np)=0;

for i=1:Np

if(i==PA) % Plotting the avalanche
%mesh(H);pause(0.01);
end

    % Dropping the new particle

    z=(Nx-1)*rand*exp(T*rand);
s(1)=Nx-round(real(z));
s(2)=Nx-round(imag(z));
    H(s(1),s(2))=H(s(1),s(2))+1;

  if(i==PA)
%mesh(H);pause(0.01);
end
```

```
    GoOn=1;
    while GoOn==1

        % Slopes
        Z=A*H+H*B;

        [S1,S2]=find(Z>Zc); % Coordinates of overcritical slopes
        Nd=length(S1); % Number of particles to drop
        if Nd==0 % If no particles to drop, exit the loop
            GoOn=0;
        else
            for j=1:Nd % Drop the particles
                H(S1(j),S2(j))=H(S1(j),S2(j))-2;
                if S1(j)>1
                    H(S1(j)-1,S2(j))=H(S1(j)-1,S2(j))+1;
                end
                if S2(j)>1
                    H(S1(j),S2(j)-1)=H(S1(j),S2(j)-1)+1;
                end
            end

    if(i==PA) % Plot the avalanche
        %mesh(H);pause(0.01);
    end

        end

        H=C.*H;

    end

    if mod(i,PI)==0
        %mesh(H); % Plot the pile
        %pause(0.001);
    %PercentDone=100*i/Np % Report on progress
    end


    M(i)=sum(sum(H)); % Mass at this time step

    % Checking for avalanches

if i>2 % Leave out the 1st step
dM=-1*M(i)+M(i-1); % Mass change * -1
if dM>0 % If an avalanche
NA=NA+1;
            ava(NA)=dM;
        end
end
```

```
end

% Plot the final pile
figure;
surfl(H);
shading interp;
title('Final pile');

% Plot mass as a function of time
figure;
plot(M);
title("Pile mass as a function of time",'FontSize',18);
xlabel('N.o. particle dropped','FontSize',18);
ylabel('Mass of the pile','FontSize',18);
zp = BaseZoom();
zp.run;

% Here we do the same procedure as with the actual experiments

min_value = min(ava);
max_value = max(ava);
num_bins = 25;
% Define the range of exponents for the logspace
exponents = linspace(log10(min_value), log10(max_value), num_bins+1);

% Calculate the bin edges
bins = 10.^exponents;
count = histc(ava, bins);

% ava cumulative increasing
figure;
subplot(1, 2, 1);
cumulative = cumsum(count);
plot(bins, cumulative/cumulative(end), '.');
hold on;
title("Cumulative avalanche distribution",'FontSize',20);
xlabel('size  [g]','FontSize',20);
ylabel('cdf','FontSize',20);

% loglog cumulative
subplot(1, 2, 2);
loglog(bins, cumulative/cumulative(end), '.');
title("Cumulative avalanche distribution on logarithmic scale",'FontSize',20);
xlabel('size  [g]','FontSize',20);
ylabel('cdf','FontSize',20);

% ava pdf
figure;

subplot(1, 2, 2);
```

```
pdf = count(1:(end-1))./(bins(2:end) - bins(1:(end-1)));
binlog = log10((bins(2:end) + bins(1:(end-1)))/2);
pdflog = log10(pdf/sum(pdf));

hold on;
loglog(binlog, pdflog, '.');

x = binlog(:,1:20);
y = pdflog(:,1:20);

inf_indexes = find(y == -Inf);

% Remove the specific point from x and y
x(:, inf_indexes) = [];
y(:, inf_indexes) = [];

title("Avalanche size probability density function on log-log scale",'FontSize',20);
f = fit(x',y', 'poly1');
plot(f,x,y,"x",'predobs');
xlabel('log (size)','FontSize',20);
ylabel('log (pdf)','FontSize',20);
legend("Datapoints", "Datapoints used for fit","Fit", "Error lines",'FontSize',15);


hold off;

subplot(1, 2, 1);
plot((bins(2:end) + bins(1:(end-1)))/2,pdf/sum(pdf), 'x');
title("Avalanche size probability density function",'FontSize',20);
ylabel('pdf','FontSize',20);
xlabel('size [g]','FontSize',20);

ci = confint(f);
Alog = f.p2
A = 10^Alog
dA = A*log(10)*abs(ci(1,2)-ci(2,2))/2
alpha = -f.p1
dalpha = abs(ci(1,1)-ci(2,1))/2
```